PHILOSOPHICAL MAGAZINE B, 1999, VOL. 79, NO. 2, 205–221

Electronic structure calculations of Al–Cu alloys: comparison with experimental results on Hume-Rothery phases

By VINCENT FOURNÉE†, IGOR MAZIN‡,
DIMITRIOS A. PAPACONSTANTOPOULOS‡ and ESTHER BELIN-FERRÉ†

†Laboratoire de Chimie Physique Matière et Rayonnement, Unité Mixte de Recherche au CNRS 7614 and Groupement de Recherche Concertation pour l'Investigation les Quasicristaux (Unité CNRS G1022)
11 rue Pierre et Marie Curie, 75231 Paris Cedex 05, France
‡Complex System Theory Branch, Naval Research Laboratory, Washington, DC 20375-5345, USA

[*Received 15 January 1998 and accepted 30 May 1998*]

ABSTRACT

Electronic band-structure calculations for a set of hypothetical Al–Cu alloys are presented. The influence of the local order and of the Cu concentration on the local density of states is analysed. The Al s states are repelled towards the bottom of the occupied band by the interaction with the more localized Cu d states lying about 4 eV below the Fermi level. Bonding and antibonding Al p states also appear, located on each side of the Cu d band. The coupling between the more extended states of Al with the d band of Cu is well described by a Fano-like effect. Two calculations performed for real Al–Cu phases of the Hume-Rothery type allow direct comparison with experimental results obtained by soft-X-ray spectroscopies. A pseudogap induced by the interaction between the Fermi sphere and the Brillouin zone is observed in agreement with the experiment. The availability of the Hume-Rothery criterion in the formation of the pseudogap observed in quasicrystalline phases is also discussed.

§1. INTRODUCTION

A large class of stable quasicrystalline phases form in Al–TM–TM′ systems where TM is a late transition metal or a noble metal (Pd or Cu) and TM′ is a transition metal such as Fe, Mn or Ru (Inoue *et al.* 1990). Perfect quasicrystalline order can be achieved with long-range atomic correlations as can be seen from the diffraction pattern (de Boissieu *et al.* 1992). High values of the electrical resistivity are found (Berger 1994) and a pseudogap at the Fermi level as has been observed by soft-X-ray emission and absorption spectroscopies as well as photoelectron spectroscopy techniques (Belin-Ferré and Dubois 1996, Stadnik *et al.* 1997). Specific heat measurements also show the low value of the density of states (DOS) at the Fermi level E_F in these icosahedral phases (Klein *et al.* 1991). The Hume-Rothery (HR) picture has been largely invoked as an explanation of the pseudogap opening because the Bragg planes associated with intense spots of their diffraction pattern are near the Fermi surface (Friedel and Denoyer 1987). The fact that icosahedral phases form along lines with constant-electron-per atom ratio (e/a) of the phase diagram also supports this idea (Dong *et al.* 1994), but this picture is not fully consistent with experimental data as it is unable to explain the behaviour of the conductivity with

temperature and structural perfection of the sample. The important role of the sp–d hybridization at E_F in the formation of the pseudogap has also been pointed out, from both experimental and theoretical grounds (Fournée *et al.* 1997).

In this paper, we present some band-structure calculations for a set of hypothetical binary Al–Cu alloys in various cubic structures and with different compositions. The aim was to analyse the trends in the changes of the Al band structure upon alloying as a function of the Cu concentration and local environment. These calculations are helpful to understand experimental results on the electronic distributions in a set of Al–Cu alloys of the HR type using soft-X-ray spectroscopies (SXSs) (Fournée *et al.* 1998). We are looking for specific features induced by the Fermi surface (FS) Brillouin zone (BZ) interaction in the recorded spectra with increasing isotropy of the BZ. We present also two band-structure calculations for two real phases where a direct comparison between the calculated and experimental electronic distributions is possible.

The paper is organized as follows: the calculation methods are presented in § 2 and the results are described and discussed in comparison with experimental data in § 3.

§ 2. Methods of calculation

We have used the augmented-plane-wave (APW) method (Matheiss *et al.* 1968) to calculate energy bands and DOSs for hypothetical alloys in the Al–Cu system. Namely, calculations have been performed for Al_2Cu and $AlCu_2$ in the fluorite structure, for Al_3Cu and $AlCu_3$ in the Cu_3Au structure and for AlCu in CsCl and NaCl structures. These APW calculations were performed self-consistently using scalar relativistic terms within the muffin-tin approximation. Exchange and correlation of the electrons are treated within the local-density approximation (LDA) using the formalism of Hedin and Lundqvist (1971). Equal sphere radii were used for Al and Cu atoms, which scale with the lattice constant. The equilibrium lattice parameters were determined by fitting the calculated total energy at various lattice constants with a least-squares fit (Birch 1978). They are listed in table 1. We have treated the highest s, p and d orbitals as valence-band (VB) levels, all other states being core levels. The band states were calculated on an equally spaced mesh in the irreducible zone of $89k$ points for the NaCl and other fcc structures and $35k$ points for sc structures. The accuracy for the total energy is of the order of 0.1 mRyd. We also have performed tight-binding (TB) linear muffin-tin orbital (LMTO) calculations (Andersen 1975, Andersen and Jepsen 1984, Skriver 1984) in the atomic sphere approximation (ASA) for $Al_{10}Cu_{10}$ and Al_4Cu_9 respectively in the monoclinic and cubic γ-brass structures. We have used the Stuttgart 4.7 code for the TB LMTO calculations.

Table 1. Crystallographic data.

Alloy (structure type)	Lattice parameter (Å)	Lattice
AlCu (NaCl)	5.013	Fcc
AlCu (CsCl)	2.914	Sc
Al_2Cu (fluorite)	6.070	Fcc
$AlCu_2$ (fluorite)	6.006	Fcc
$AlCu_3$ (Cu_3Au)	3.607	Sc
Al_3Cu (Cu_3Au)	3.866	Sc

For $Al_{10}Cu_{10}$, the lattice parameters are $a = 12{\cdot}066$ Å, $b = 4{\cdot}105$ Å, $c = 6{\cdot}913$ Å and $\beta = 124{\cdot}96^{\circ}$ with the space group $C2/\underline{m}$. There are 20 atoms in the unit cell. The γ-brass structure is sc with space group $P\bar{4}3m$ and lattice parameter $a = 8{\cdot}7027$ Å. The unit cell contains 52 atoms and can be viewed as $3 \times 3 \times 3$ CsCl distorted cubes, with formula unit $Al_{16}Cu_{36}\square_2$ ($\square$ is a vacancy site) (Dong 1996). In $Al_{10}Cu_{10}$ we used Al atomic spheres with $r = 1{\cdot}49$ Å and for Cu with $r = 1{\cdot}38$ Å. For both Al and Cu we used s, p and d orbitals. To achieve better filling of the open $C2/m$ structure of $Al_{10}Cu_{10}$ we used four large empty spheres ($r = 1{\cdot}01$ Å) per formula unit and 12 smaller empty spheres ($r = 0{\cdot}64$ Å). For the former we include s, p and d and for the latter s and p orbitals. For Al_4Cu_9 we were able to achieve satisfactory filling without using empty spheres. We used atomic spheres of similar sizes ($r = 1{\cdot}54$-$1{\cdot}65$ Å) for all atoms and kept s, p and d orbitals on all sites. For both compounds we used up to $10 \times 10 \times 10$ mesh in the BZ, which resulted in 76 irreducible k points for Al_4Cu_9 and 282 for the lower symmetry $Al_{10}Cu_{10}$.

The last two alloys are real phases and are among the Al–Cu alloys of the HR-type that we have investigated by means of soft-X-ray emission and absorption spectroscopies (Fournée *et al.* 1998). These allow one to probe separately the electronic distributions around each type of atom with a given symmetry. The recorded intensities are

$$I(E) \approx |M|^2 \mathcal{N}(E) * \mathcal{L}(E), \tag{1}$$

where M is the dipolar matrix element of the X-ray transition probability, $\mathcal{N}(E)$ is the partial DOS and $\mathcal{L}(E)$ is a Lorentzian function whose full width at half-maximum (FWHM) is the energy width of the inner level involved in the X-ray transition (Agarwal 1979). For a meaningful comparison with the experimental spectra, plots of the DOS have been broadened with a Lorentzian to account for the inner level involved in the X-ray transition and for the spectrometer window. We did not calculate the matrix element of the dipolar transition between the valence state and the core states, assuming that it is a smooth function of the energy over the width of a band (McCaffrey and Papaconstantopoulos 1974). For the Al $L_{2,3}$ spectra, we have added the s DOS with two fifths of the d DOS, following the prescription of Goodings and Harris (1969). As no absolute values of the DOS can be derived from these techniques, all the spectra are normalized to their maximum intensity and are presented in arbitrary units.

§3. Results

The total and the site and angular momentum decomposed DOSs are presented in figures 1–6. The Cu d states are the dominant states for all alloys. They form a set of peaks at about 4 eV from the Fermi level E_F which is lower than in pure Cu by approximately 1 eV. The width of the Cu d band is reduced compared with that of pure Cu. These effects strongly depend on the coordination of the Cu atoms. The width of the band decreases in the alloys as the Cu–Cu coordination number is reduced and the interatomic distances increase. Table 2 gives the coordination number of different atoms in various alloys. For example, the width is 3.8 eV in Cu fcc where an atom is surrounded by 12 Cu atoms at a distance of 2.55 Å and it is reduced to 2.9 eV in Cu_3Al where the number of Cu nearest neighbours is eight at the same distance. It reaches a minimum of 0.5 eV in the case of Al_2Cu in the fluorite structure where a Cu atom is at the centre of a first shell occupied only by eight Al atoms at 2.6 Å, the next 12 Cu atoms being located on a second shell at 4.2Å.

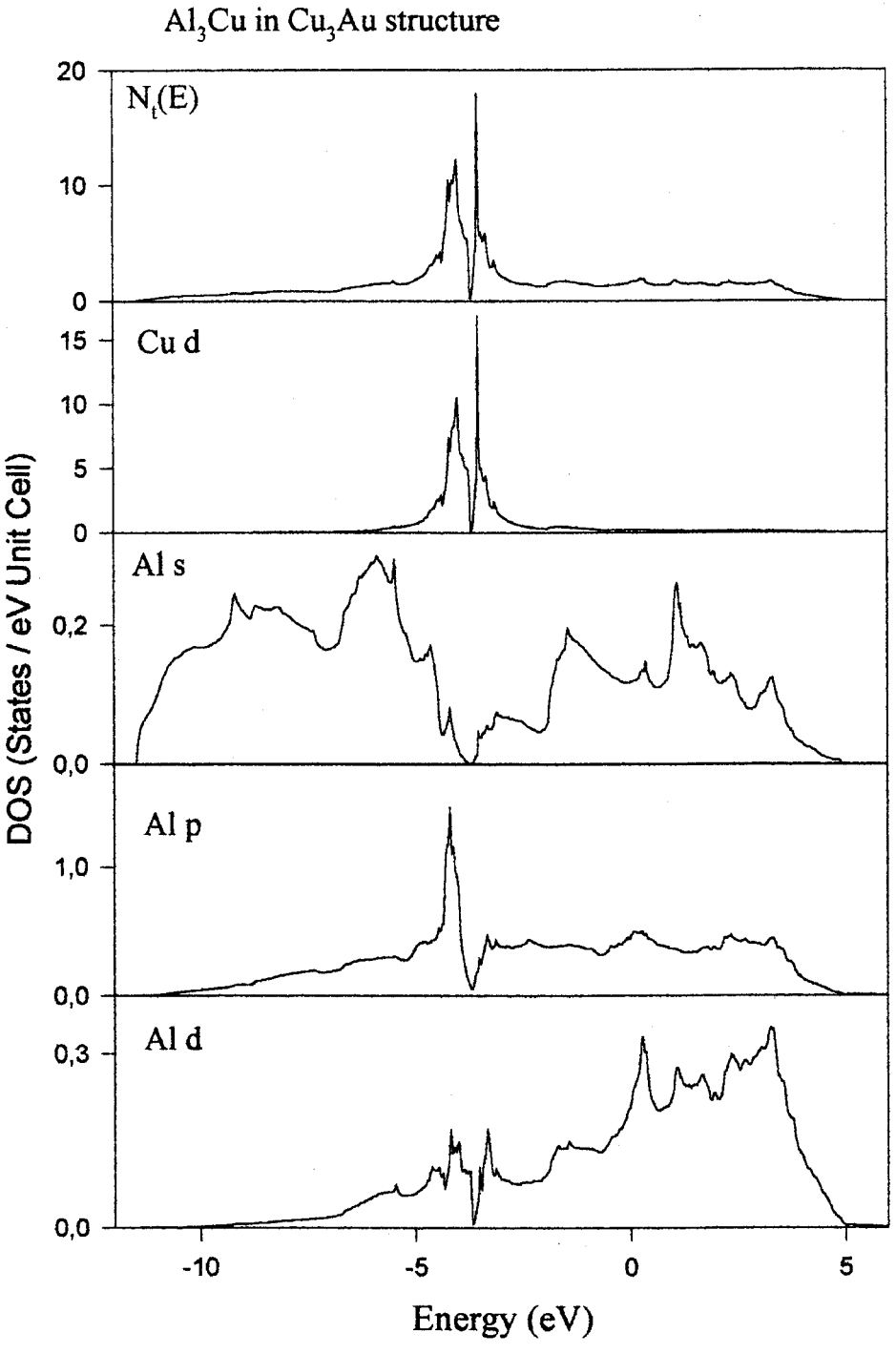

Figure 1. Calculated total and partial DOSs of Al_3Cu in the Cu_3Au structure: from top to bottom the total DOS, Cu d, Al s, Al p and Al d distributions.

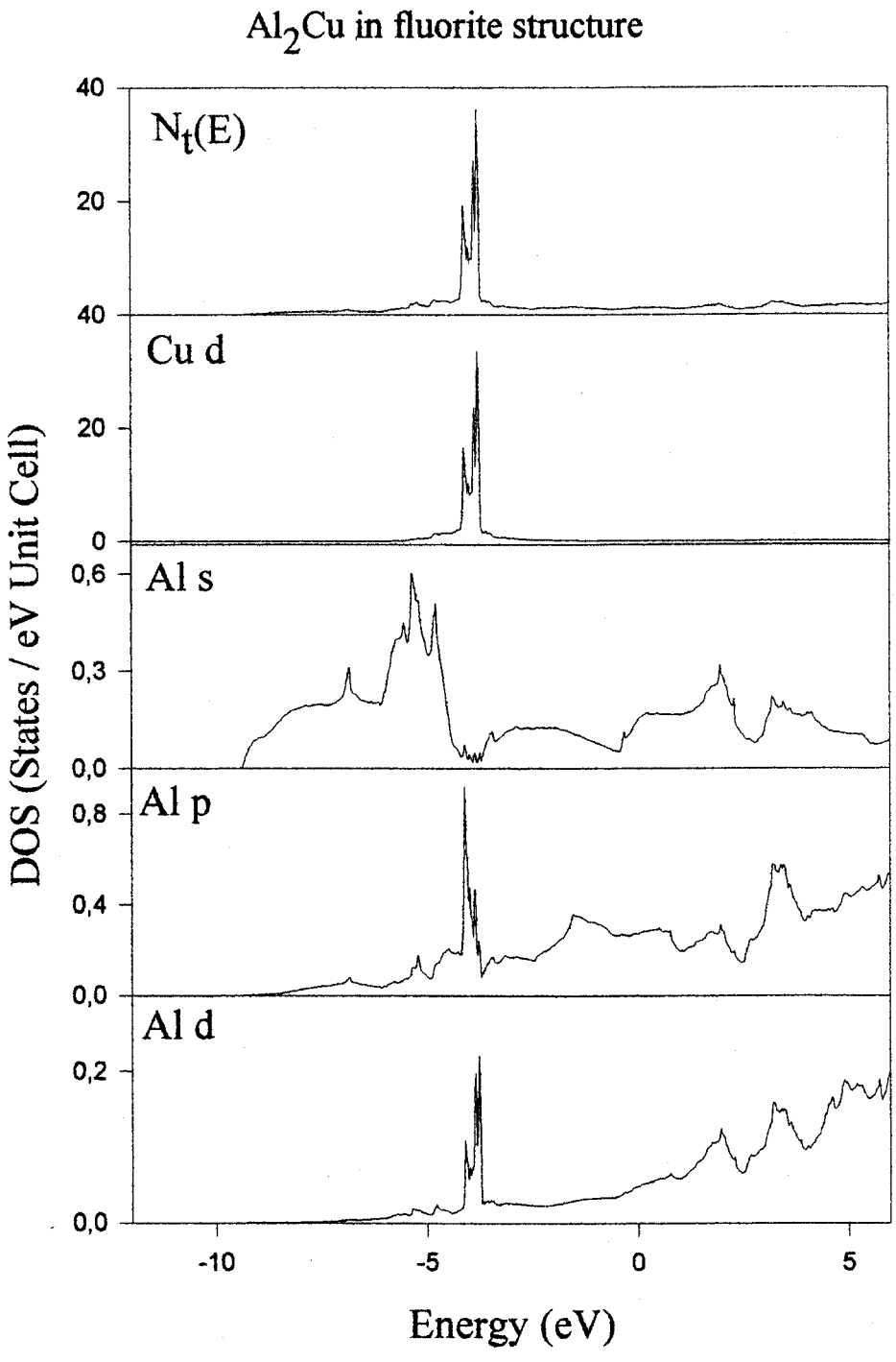

Figure 2. Calculated total and partial DOSs of Al_2Cu in the fluorite structure: from top to bottom the total DOS, Cu d, Al s, Al p and Al d distributions.

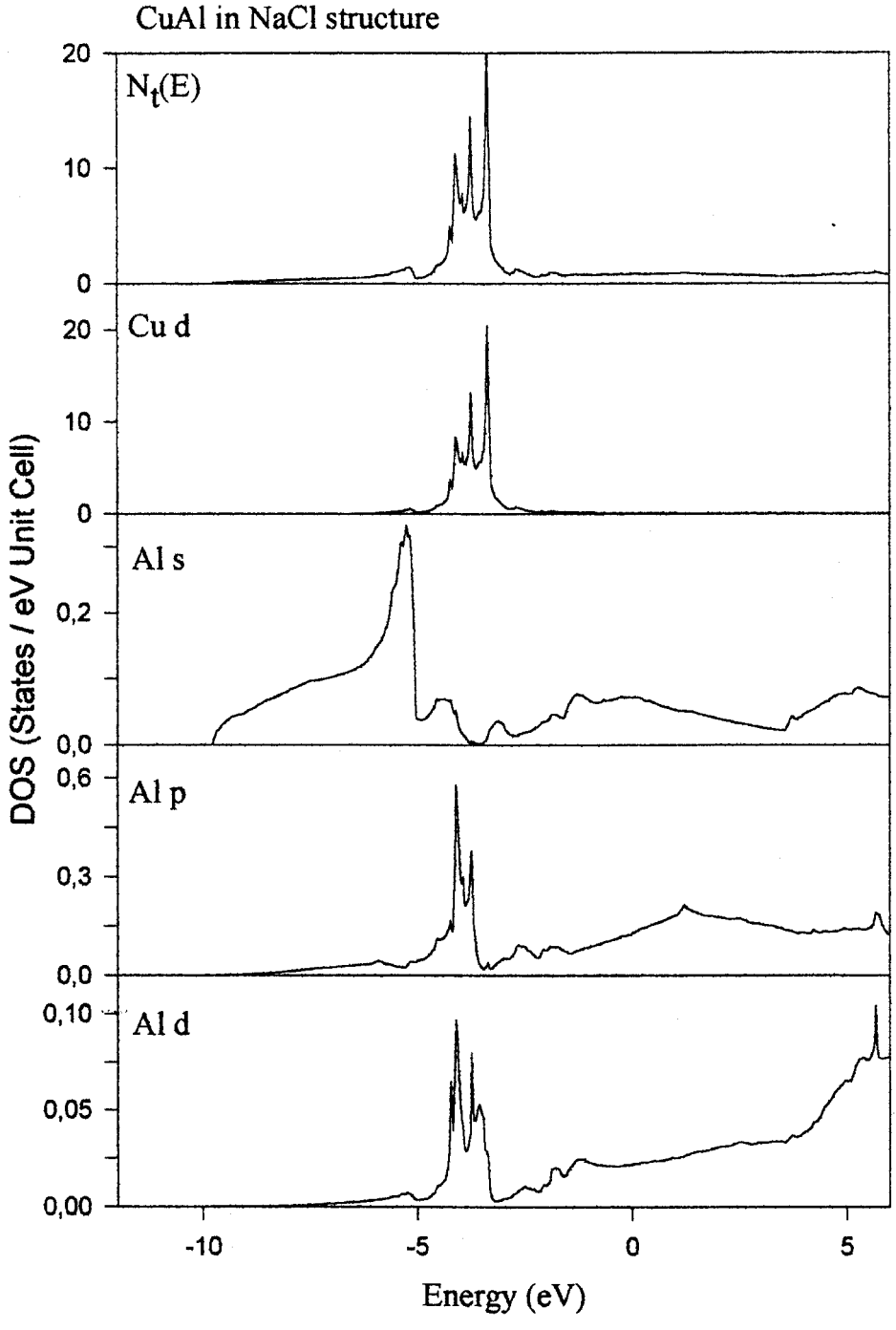

Figure 3. Calculated total and partial DOSs of AlCu in the NaCl structure: from top to bottom the total DOS, Cu d, Al s, Al p and Al d distributions.

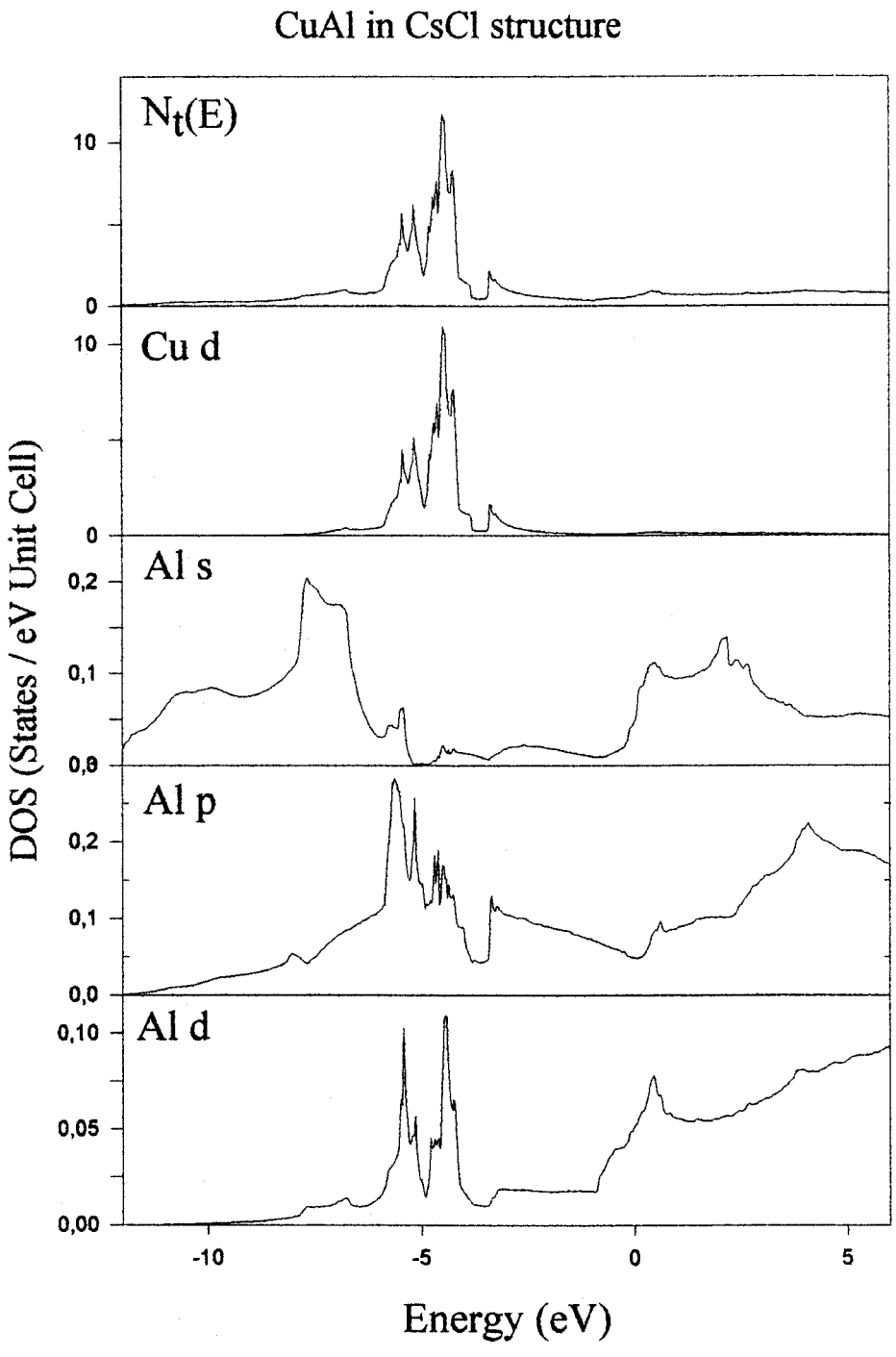

Figure 4. Calculated total and partial DOSs of AlCu in the CsCl structure: from top to bottom the total DOS, Cu d, Al s, Al p and Al d distributions.

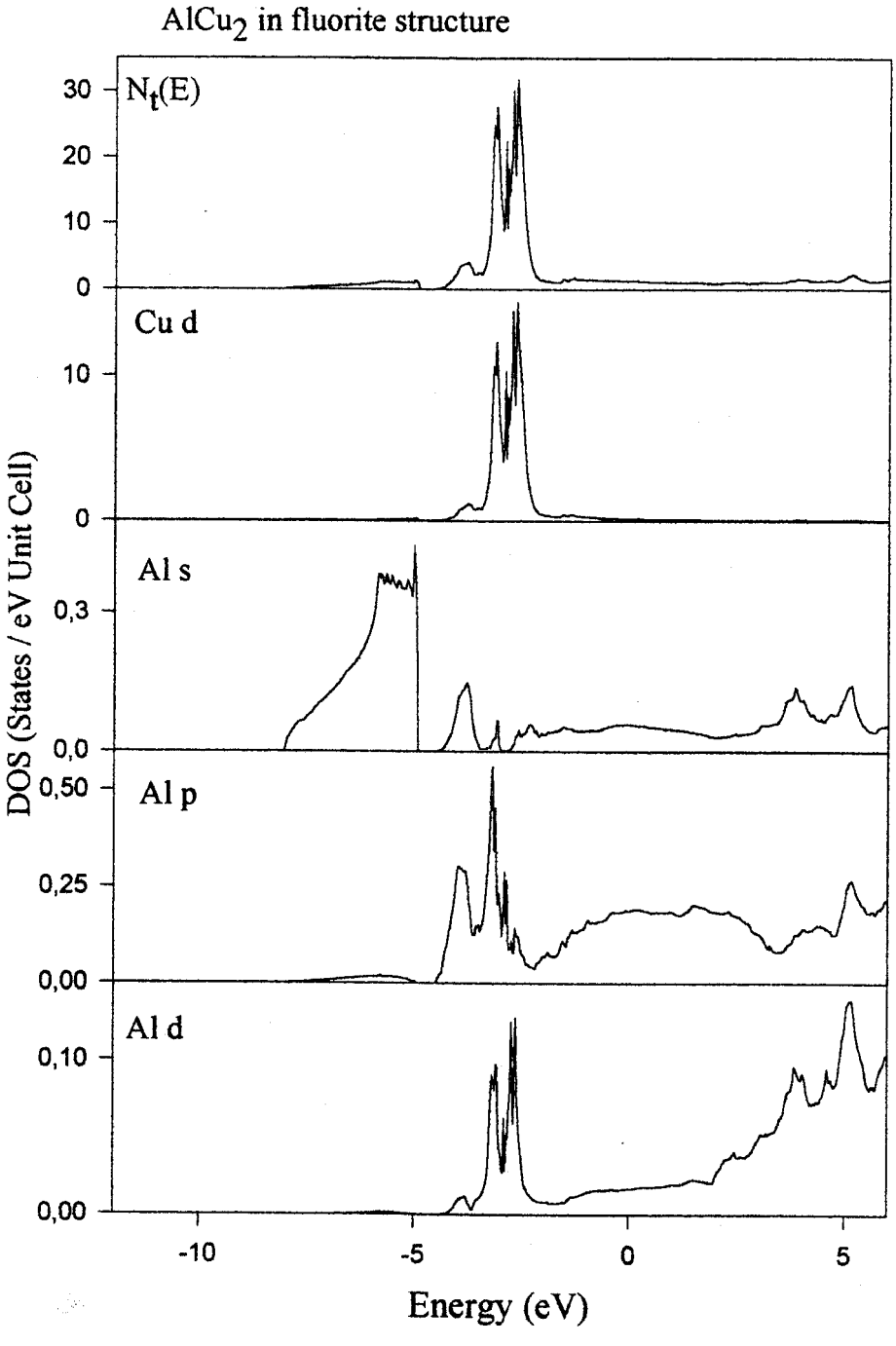

Figure 5. Calculated total and partial DOSs of $AlCu_2$ in the fluorite structure: from top to bottom the total DOS, Cu d, Al s, Al p and Al d distributions.

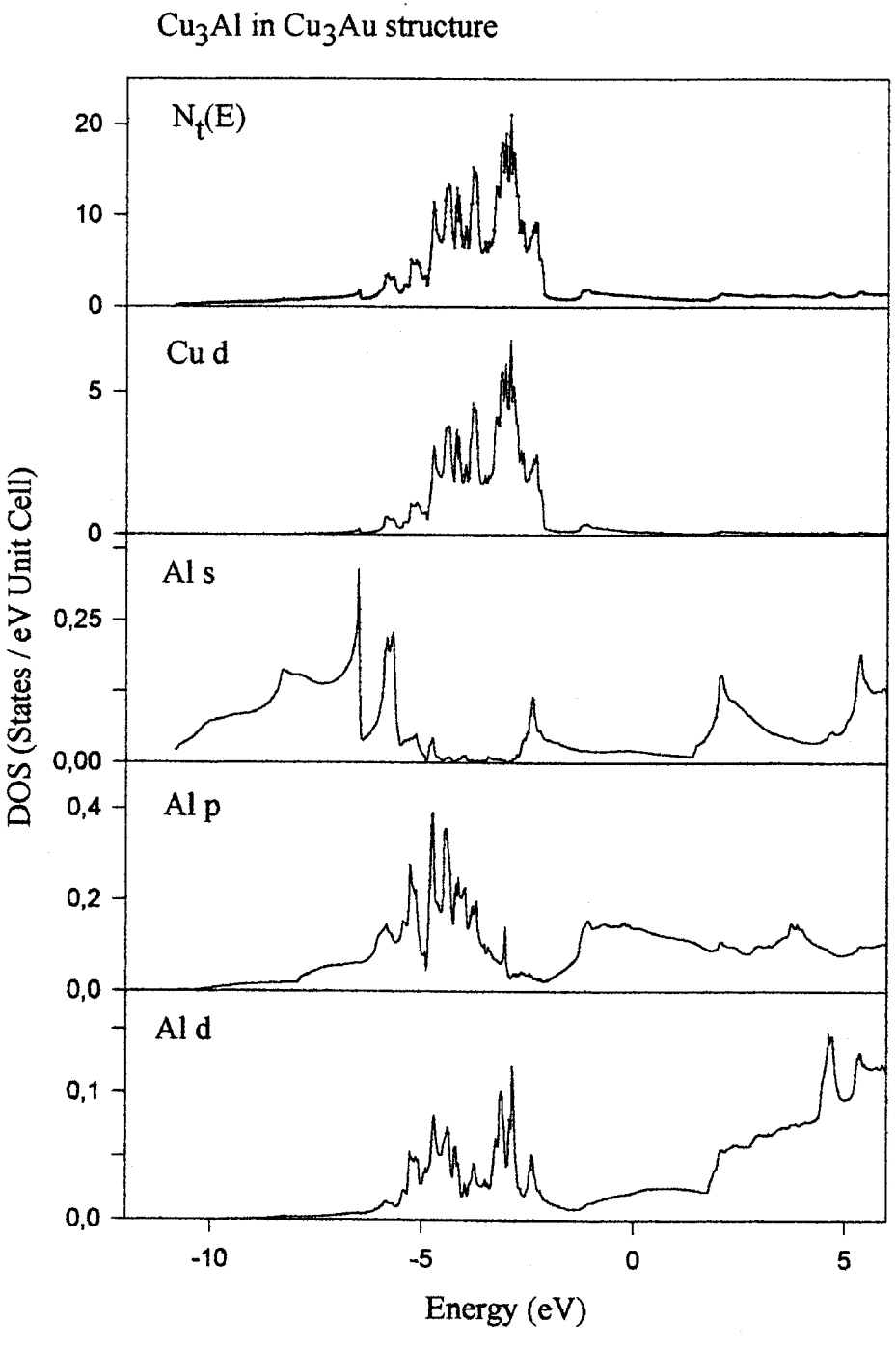

Figure 6. Calculated total and partial DOSs of $AlCu_3$ in the Cu_3Au structure: from top to bottom the total DOS, Cu d, Al s, Al p and Al d distributions.

Table 2. Coordination numbers around the elements.

Alloy	Atom	Coordination number N	Distance (Å)
Al_4Cu_9	Al–Cu	9–11	2.5–2.8
	Al–Al	0–3	2.5–2.8
	Cu–Al	3–6	2.5–2.8
	Cu–Cu	6–9	2.5–2.8
$Al_{10}Cu_{10}$	Al–Cu	6–8	2.4–3.0
	Al–Al	3–6	2.5–2.8
	Cu–Al	6–7	2.5–2.8
	Cu–Cu	4–5	2.4–2.9
$AlCu_2$	Al–Cu	8	2.6
	Al–Al	12	4.2
	Cu–Al	4	2.6
	Cu–Cu	6	3.0
AlCu (NaCl)	Al–Cu/Cu–Al	6	2.5
	Al–Al/Cu–Cu	12	3.5
AlCu (CsCl)	Al–Cu/Cu–Al	8	2.5
	Al–Al/Cu–Cu	6	2.9
Al_3Cu	Al–Cu	4	2.75
	Al–Al	8	2.75
	Cu–Al	12	2.75
	Cu–Cu	6	3.85
$AlCu_3$	Cu–Al	4	2.55
	Cu–Cu	8	2.55
	Al–Cu	12	2.55
	Al–Al	6	3.6
Al_2Cu	Cu–Al	8	2.6
	Cu–Cu	12	4.2
	Al–Al	6	3.0
	Al–Cu	4	2.6
Cu(fcc)	Cu–Cu	12	2.55

Band narrowing is a consequence of the decrease in the d–d hopping amplitudes and of the number of hopping channels. It is well known that the band width grows with the number Z of the nearest neighbour as $Z^{1/2}$. In the TB theory the second moment of the partial DOS at site i given by

$$M_2 = \left(\int N(E)E^2\,\mathrm{d}E\right) \Big/ \left(\int N(E)\,\mathrm{d}E\right) \tag{2}$$

is defined by the sum $\sum t_{ij}^2$ over all neighbours j, where t_{ij} is the hopping amplitude between sites i and j. Since the bandwidth is of the order of $M^{1/2}$, adding more Cu–Cu bonds of a given length leads to the corresponding square-root growth of the bandwidth, as can be seen from figures 1–6.

On the other hand since the position of the d band is determined by its interaction with the Al band, the shift of the d band towards high binding energies is more sensitive to the Cu–Al coordination number and distance. An example is the larger shift observed for the CsCl structure than for the NaCl structure, because a Cu atom has more Al neighbours (eight instead of six at 2.50 Å).

Another interesting point is the opening of a pseudogap at the edge of the Cu d band in some of the alloys. It is particularly obvious in the case of $AlCu_3$ and AlCu

in the Cu_3Au and CsCl structures respectively. The Cu s and p DOSs are very small and should not contribute significantly to the Cu site decomposed DOS.

Concerning the Al site decomposed DOS with s, p and d symmetries, one can see that they are not smooth functions of energy as they would be in a free-electron system. Common features for all alloys can be outlined as follows: firstly the strong enhancement of the Al s partial DOS at high binding energies followed by a minimum in the energy range of the Cu d band; secondly the splitting of the Al p partial DOS into two parts located on each side of the Cu d states; thirdly the appearance of coinciding Al d-like and Cu d states.

All these features can be interpreted as the effect of the coupling between a broad conduction band and a localized d band. The deformation of the conduction band has been described theoretically by Terakura (1977) in terms of a Fano effect. Namely, Al 3s and 3p electrons form bonding and antibonding states located on each side of a dip. These energy positions correspond to the top of the Cu 3d localized states, owing to mutual repulsion of the two states. This is clearly seen in the case of AlCu in the CsCl structure (figure 4). The Al 3s DOS is largely enhanced at high binding energies, the bonding peak around 7 eV is well defined, and for higher energies the DOS almost vanishes, showing that the antibonding states are almost empty. Consequently, the bottom of the VB has an almost pure s character. The Al 3p DOS splits into bonding and antibonding states located on each side of a dip, at 3.6 eV below the Fermi level, which corresponds to that observed at the top of the Cu d band. Some d-like states appear also in the Al site decomposed DOS, reproducing the shape of the Cu d band at the same energy but with a very low intensity. This is very similar to the Fano effect, well known in Raman spectroscopy.

We can compare these results on hypothetical alloys with spectroscopic measurements of the electronic distributions in real phases. We present in figure 7 the calculated spectra for AlCu with a CsCl structure, which are quite realistic, and the experimental spectra obtained for the monoclinic $Al_{10}Cu_{10}$. The Al Kβ spectrum corresponds to transitions between Al 3p states and the Al 1s core hole. Thus, we have convoluted the calculated Al p DOS with a Lorentzian with FWHM equal to 0.42 eV, which is the natural width of the Al 1s level (Krause and Oliver 1979), and we have then broadened it by an experimental Gaussian function with a FWHM equal to 0.3 eV. The Al $L_{2,3}$ spectrum results from transitions between Al 3s, d states and the Al $2p_{3/2}$ core hole, which has a natural width of 0.004 eV. Here, the main broadening comes from the experimental resolution: a Gaussian with a FWHM equal to 0.3 eV. The Cu Lα spectrum results from transitions between Cu 3d, 4s states and the Cu $2p_{3/2}$ core hole. Essentially, it reflects the occupied 3d distribution because the probability of a d–p transition is much higher than that of an s–p transition. In addition, the contribution of the s states to the occupied band is already faint in the pure metal (Papaconstantopoulos 1986). The Cu d DOS has been broadened by a Lorentzian with a FWHM equal to 0.56 eV (natural width of the Cu $2p_{3/2}$ level) and by a Gaussian with a FWHM equal to 0.4 eV. As noted in § 2, all the spectra are normalized to the same value. We find agreement between theoretical and experimental curves concerning the position of the peaks and the trends in the band deformation. The Cu d states lie at about 4 eV below E_F. The structures observed on the low-binding-energy side of the experimental curve are satellite emissions and do not correspond to any structure of the DOS. The splitting of Al p and Al s,d distributions in the bonding and antibonding peaks located on both sides of the Cu d band is confirmed. However, some discrepancies appear in the

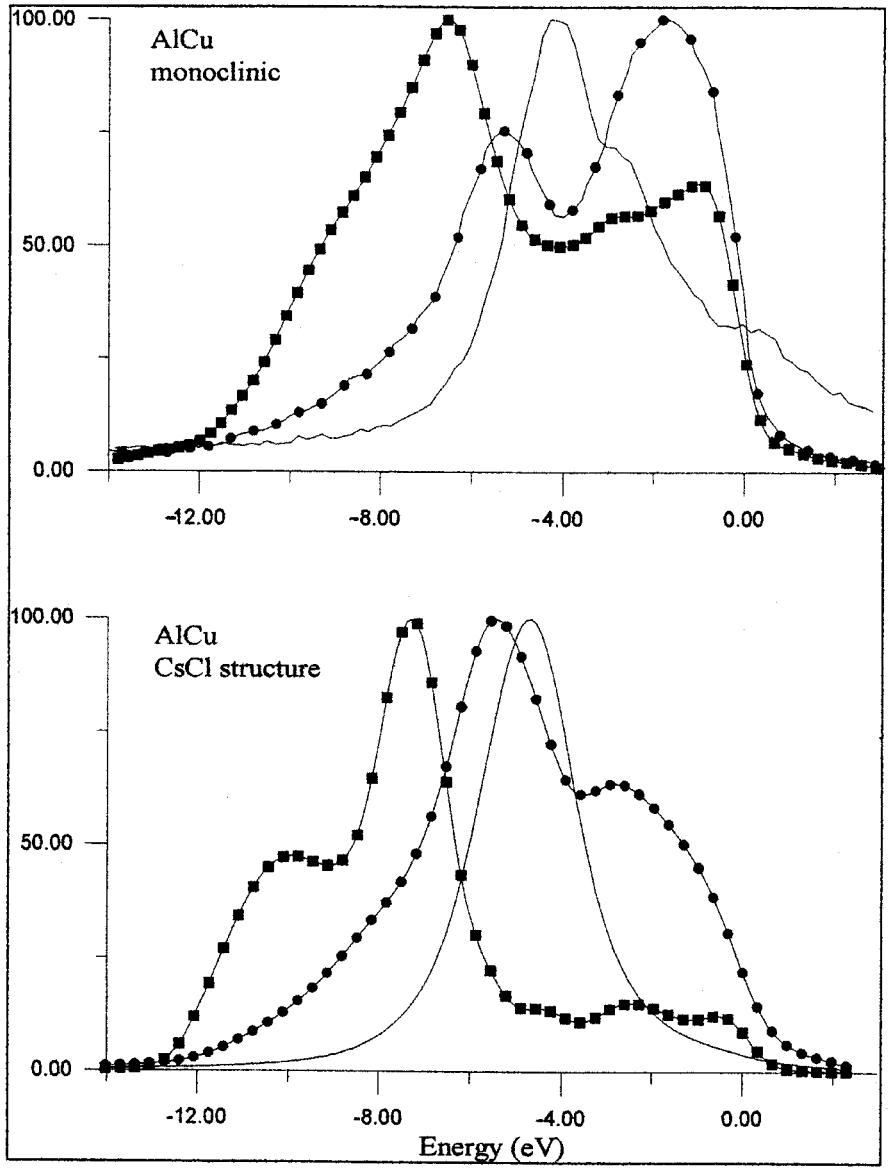

Figure 7. (*a*) Experimental Al s,d (■), Al p (●) and Cu d (——) distributions in the $Al_{10}Cu_{10}$ monoclinic phase. (*b*) Calculated Al s,d (■), Al p (●) and Cu d (——) distributions for the AlCu in the CsCl structure.

relative intensities of these two peaks. The contribution to the intensity of the high-binding-energy side of the VB seems to be overestimated in the calculation. A possible explanation could be that the variation in the matrix element of the transition is not the smooth function of the energy that we have assumed and, therefore, should be taken into account to obtain a better agreement.

We turn now to the results obtained for $Al_{10}Cu_{10}$ and Al_4Cu_9 real phases for which we have performed a TB LMTO ASA calculation. These alloys are of the HR

type; Al and Cu atoms have a small difference between their atomic radii and electronegativities: They have an electron-per-atom ratio such that the Fermi wave-vector k_F just touches a BZ boundary, that is satisfies the $k_F \approx K/2$ condition, where K is a reciprocal-lattice vector.

The samples were prepared using 99.95% pure elements. These were melted in an induction furnace under an Ar atmosphere. Further annealing were performed to obtain single-phase alloys. The characterization of the phases was achieved by X-ray diffraction experiments. The BZ of the monoclinic $Al_{10}Cu_{10}$ alloy is a 24-face polyhedron. The BZ of the Al_4Cu_9 γ-brass structure is more spherical (36-face polyhedron) and is associated with strong Bragg peaks, suggesting a strong structure factor. This last phase was the most promising for studying the effect of the FS–BZ interaction on the opening of a structure-induced pseudogap in the DOS.

The partial DOS, the calculated spectra and the corresponding experimental spectra are presented in figures 8 and 9 for $Al_{10}Cu_{10}$ and Al_4Cu_9 respectively. We shall not discuss further the changes in the sp DOS in these alloys as it follows the same trends already described in the previous paragraph.

Concerning the peak position and bandwidth, good agreement is found between the calculated and experimental spectra for both alloys. A slight shift of about 0.4 eV towards the Fermi level is seen in the position of the calculated Cu d position compared with experiment which is a well known consequence of the spurious self interaction in the LDA. The appearance of Al d states in coincidence with Cu d states explains well the feature observed in the Al $L_{2,3}$ spectra at about 4 eV below E_F, between the bonding and antibonding peaks in figure 9. The calculated Al p distributions are also slightly displaced towards the Fermi level, and the distance between the bonding and antibonding peak is lower than the observed value. For example, it is 3.7 eV for Al_4Cu_9 in the experiment and only 2.9 eV in the calculation. We once again observe the same discrepancy as in the APW calculations, that is the relative intensities of the two peaks are reversed in the calculations as compared with the experiment.

A shallow minimum is seen in the sp DOS at the Fermi level for $Al_{10}Cu_{10}$. For this low-symmetry structure, several planes verify approximately the $K \approx 2k_F$ condition. The pseudogap is much deeper in the case of Al_4Cu. It arises from the opening of a gap at the 411 and 330 faces of the Brillouin zone, their multiplicities being 24 and 12 respectively. Assuming valences of +3 and +1 for Al and Cu, the free-electron value of the electronic density is $n = 0{\cdot}127\ \text{Å}^{-3}$ electrons and the Fermi vector is

$$k_F = 1{\cdot}55\ \text{Å}^{-1} \approx \frac{|K_{411}|}{2} = \frac{|K_{330}|}{2} = 1{\cdot}53\ \text{Å}^{-1}.$$

Because of the high multiplicity of these vectors, a large part of the Fermi sphere develops a gap and the resulting pseudogap is much stronger for the complex cubic phase than for the monoclinic phase. The width of the pseudogap depends on the strength of the component V_K of the pseudopotential and its value is about 1 eV in this case. In the Al p experimental distribution as well as in the corresponding calculated spectra, the intensity $I(E_F)$ at E_F represents less than 40% of its maximum in the γ-brass structure instead of 50% in pure fcc Al. Thus, a small pseudogap is observed experimentally, which is due to the FS–BZ interaction but is somewhat smeared out by the effect of the broadening inherent to SXSs. Similar experimental investigations on Al–Cu alloys of the HR type have shown only slight changes in this

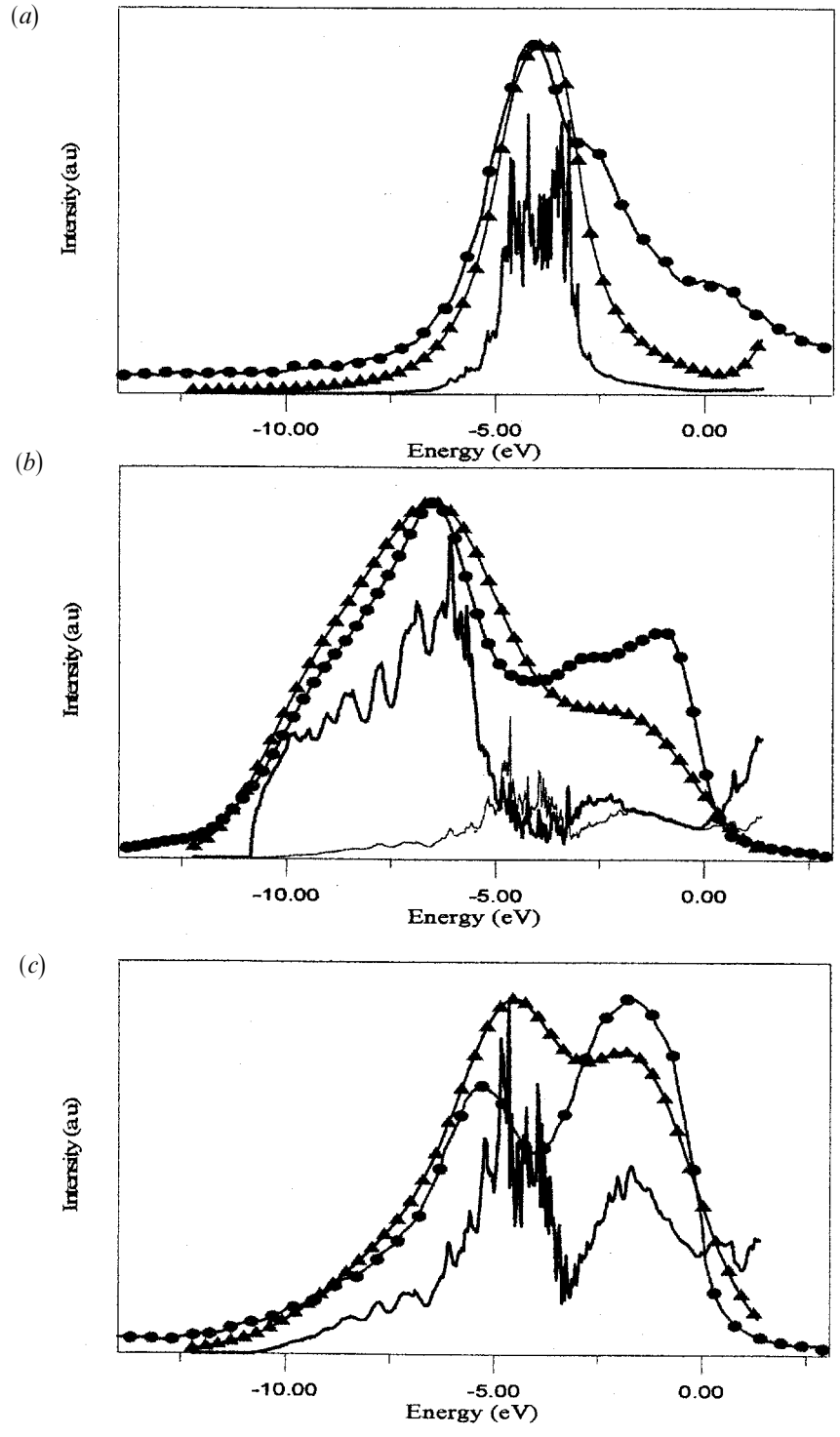

Figure 8. Partial (——) and broadened (-▲-) DOSs compared with the experimental spectra (-●-) for the $Al_{10}Cu_{10}$ alloy (au, arbitrary units) (*a*) Cu d (CuLα); (*b*) Al s (——) and Al d (——) (Al Lα); (*c*) Al p (Al Kβ).

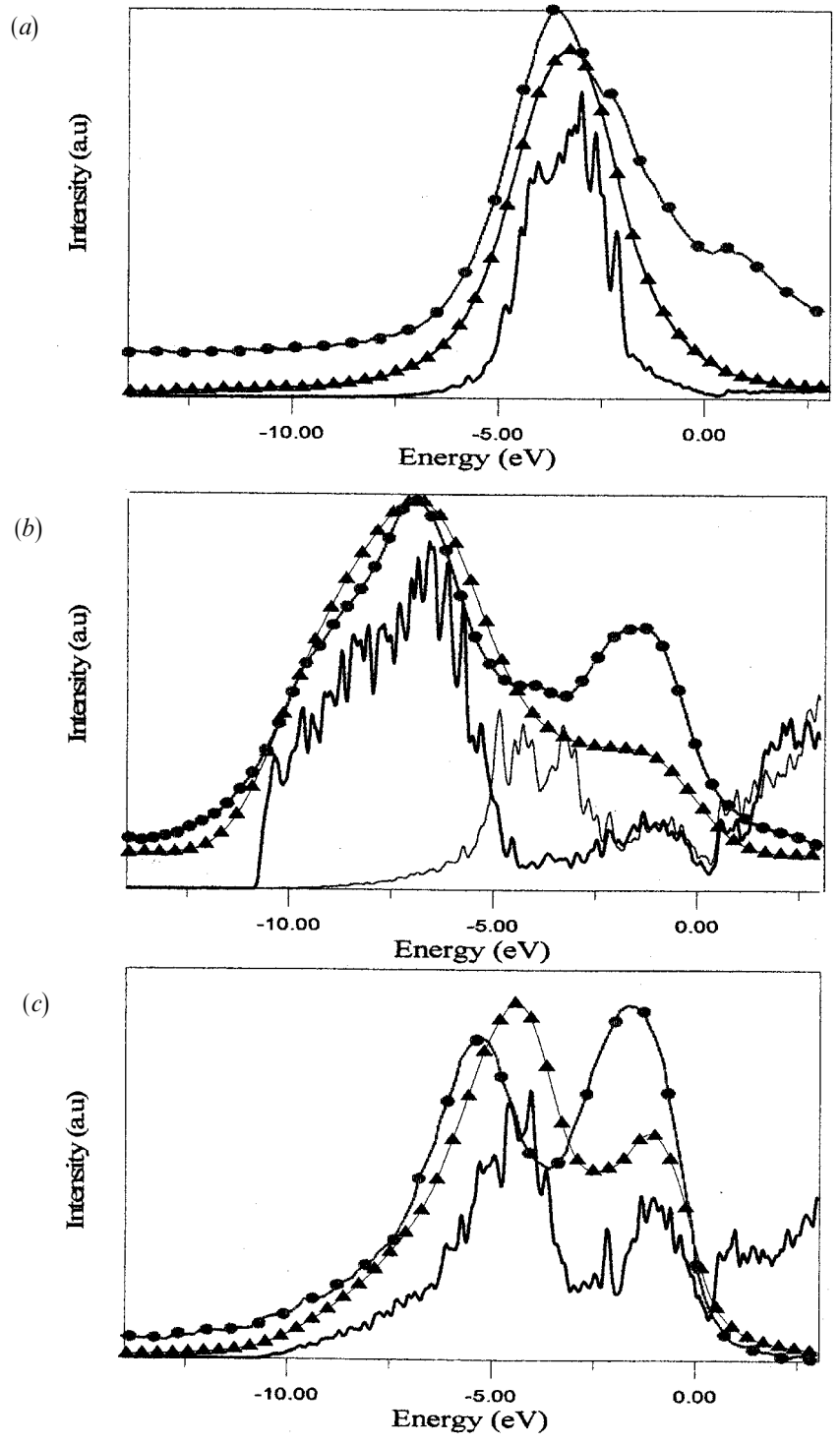

Figure 9. Partial (——) and broadened (-▲-) DOSs compared with the experimental spectra (-●-) for the Al_4Cu_9 (au, arbitrary units): (*a*) Cu d (Cu Lα); (*b*) Al s (——) and Al d (——) (Al Lα): (*c*) Al p (Al Kβ).

parameter $I(E_F)$ with increasing isotropy of their BZ. Previous SXS measurements of the electronic distributions in quasicrystalline alloys have shown a much larger reduction of $I(E_F)$ in the Al p states. For example, in the icosahedral Al–Cu–Fe phase, $I(E_F)$ drops by 70%. A more spherical pseudo BZ allows better matching with the FS and a larger pseudogap should result, but the difference in the sphericity of the two BZs (36 faces in the case of Al_4Cu_9 and 42 faces for icosahedral Al–Cu–Fe) is too small to account for such a difference in $I(E_F)$. This stresses the importance of the TM d states located near E_F that push back the Al states from the Fermi level via sp–d hybridization in Al–TM–TM′ quasicrystals. Theoretical calculations for binary Al–TM alloys (Trambly de Laissardiére *et al.* 1995) performed with and without sp–d hybridization have shown that the effect of the TM d states is to increase the magnitude of the potential diffracting the Fermi electrons and thus increases the width of the pseudogap.

§4. Conclusion

We have analysed modifications of the electronic DOS under the influence of the local environment and of the concentration in a set of hypothetical Al–Cu alloys. The interaction between the extended sp Al states and the rather localized Cu d states about 4 eV below E_F is well described by a model of the Fano type. These calculations are in good agreement with experimental results on the electronic distributions obtained by soft X-ray emission spectroscopy for a set of Al–Cu alloys of the HR type. The calculated DOS for two of these real phases allows direct comparison with experimental curves. Our results show that the FS–BZ interaction leads to the formation of a pseudogap at E_F that is observed experimentally. It stresses also the importance of the sp–d hybridization at E_F by increasing the diffracting potential and making the pseudogap more pronounced.

Acknowledgements

The motivation of the present work is based upon discussions with Dr J. M. Dubois; we are grateful to him. We thank Z. Dankhazi for his collaboration with the measurements. The experimental work has been supported in part by the Austrian Ministry of Research, East West Cooperation program, under the title 'Soft X-ray spectroscopy of metallic systems.' The hospitality offered to V.F. by the Naval Research Laboratory (Washington, DC, USA) and to V.F. and E.B.F. by the Technical University of Vienna (Austria) is warmly acknowledged.

References

Agarwal, B. K., 1979, *X-ray Spectroscopy,* Springer Series in Optical Sciences, Vol. 15 (Berlin: Springer).

Andersen, O. K., 1975, *Phys. Rev.* B, **12**, 3060.

Andersen, O. K., and Jepsen, O., 1984, *Phys. Rev. Lett.,* **53**, 2571.

Belin-Ferré, E., and Dubois, J. M., 1996, *J. Phys.: condens. Matter.,* **8**, L717.

Berger, C., 1994, *Lectures on Quasicrystals*, edited by F. Hippert and D. Gratias (Les Ulis: Les Editions de Physique), p. 463.

Birch, F., 1978, *J. geophys. Res.,* **83**, 1257.

de Boissieu, M., Durand-Charre, M., Bastie, P., Carabelli, A., Boudard, M., Bessiére, M., Lefebvre, S., Janot, C., and Audier, M., 1992, *Phil. Mag. Lett.,* **65**, 147.

Dong, C., 1996, *Phil. Mag.* A, **73**, 1519.

Dong, C., Perrot, A., Dubois, J. M., and Belin, E., 1994, *Mater. Sci. Forum,* **150–151**, 403.

Fournée, V., Belin-Ferré, E., Trambly, de Laissardiére, G., Sadoc, A., Volkov, P., and Poon, S. J., 1997, *J. Phys.: condens. Matter,* **9**, 7999.

Fournée, V., Belin-Ferré, E., and Dubois, J. M., 1998, *J. Phys.: condens. Mater*, **10**, 4231.
Friedel, J., and Dénoyer, F., 1987, *C. R. hebdd. Séanc. Acad. Sci. Paris, Ser. II,* **305**, 171.
Goodings, D. A., and Harris, R., 1969, *J. Phys.* C, **2**, 1808.
Hedin, L., and Lundqvist, B. I., 1971, *J. Phys.* C, **4**, 2064.
Inoue, A., Tsai, A. P., and Masumoto, T., 1990, *Quasicrystals,* edited by T. Fujiwara and T. Ogawa (Berlin: Springer), p. 80.
Klein, T., Berger, C., Mayou, D., and Cyrot-Lackmann, F., 1991, *Phys. Rev. Lett.,* **66**, 2907.
Krause, M. O., and Oliver, J. H., 1979, *J. phys. chem. Ref. Data,* **8**, 329.
McCaffrey, J. W., and Papaconstantopoulos, D. A., 1974, *Solid St. Commun.,* **14**, 1055.
Matheiss, L. F., Wood, J. H., and Switendick, A., 1968, *Methods in Computational Physics,* Vol. 8, edited by A. Adler, S., Fernbach, R., Rotenberg, R., (New York: Academic Press).
Papaconstantopoulos, D. A., 1986, *Handbook of the Band Structure of Elemental Solids* (New York: Plenum).
Skriver, H. L., 1984, *The LMTO Method* (New York: Springer).
Stadnik, Z. M., Purdie, D., Garnier, M., Baer, Y., Tsai., A. P., Inoue, A., Edagawa, K., Takeuchi, S., and Buschow, K. H. J., 1997, *Phys. Rev.* B, **55**, 10938.
Terakura, K., 1977, *J. Phys.* F, **7**, 1773.
Trambly de Laissardiére, G., Nguyen Manh, D., Magaud, L., Julien, J. P., Cyrot-Lackmann, F., and Mayou, D., 1995, *Phys. Rev.* B, **52**, 7920.